J. Fluid Mech. (1969), *vol.* 37, *part* 4, *pp.* 657–670
Printed in Great Britain

Stokes flow around a circular cylindrical post confined between two parallel plates

By J. S. LEE AND Y. C. FUNG

Department of Aerospace and Mechanical Engineering Sciences,
University of California, San Diego

(Received 21 October 1968 and in revised form 9 January 1969)

A slow viscous flow around a circular cylindrical post confined between two parallel flat plates is analyzed. The solution is given in the form of a series each term of which satisfies the equations of motion and continuity as well as the no-slip condition on the plates. A number of arbitrary constants left open in the series can then be determined according to the no-slip condition at the surface of the cylinder. Numerical results are presented. The series is found to be adequate when the ratio of the distance between the plates and the diameter of the post is not much larger than unity. The coefficient of resistance of the flow decreases rapidly as the sheet-thickness-to-post-diameter ratio increases. It is shown that the series converges rapidly when the thickness ratio is small, so that an approximate solution consisting of the two leading terms of the series, gives a reasonable representation of the velocity field and a good approximation to the flow resistance.

1. Introduction

This paper is concerned with the flow of a viscous incompressible fluid around a circular cylindrical post confined between two parallel flat plates (see figure 1). The motivation of the investigation comes from the study of blood flow in the smallest structural unit of the lung. It was proposed by Sobin & Fung (1967) that the capillary blood vessels in the alveoli of the lung are best described not as tubes, but as forming a 'sheet', so that the alveolar blood flow is a flow between two parallel membranes interposed with many posts. The Reynolds number of such a flow in the pulmonary alveoli is of the order of 10^{-4} to 10^{-2}; hence the convective inertia force may justifiably be neglected. Fung & Sobin (1969) presented a simplified analysis of the pulmonary blood flow in the alveoli, and demonstrated the usefulness of the approach. Also, Lee & Fung (1968) presented the results of model experiments on sheet flow. However, a more exact mathematical treatment is needed. It is the purpose of this paper to present the first step towards an analysis of the flow between two parallel plates interposed with a regular array of posts.

The problem, of course, is an old one. In 1898, Hele-Shaw discovered that the streamlines of this sort of flow can be used to represent the lines of force around a metal cylinder in a dielectric medium in a magnetic field. Using immiscible

coloured dye as an indicator, Hele-Shaw obtained a set of beautiful pictures of the streamlines around cylinders of various shapes. A little later in the same year, Stokes proved mathematically that, when the convective acceleration is neglected and the plates are very close to each other, the stream function for the velocity averaged across the thickness is governed by a two-dimensional Laplace equation. Thus the viscous flow around a cylinder between two closely spaced plates has the same streamlines as a potential flow of an inviscid fluid around a similar cylinder of infinite length. However, as a potential flow cannot satisfy the no-slip condition on the surface of the cylinder, the analogy is not complete.

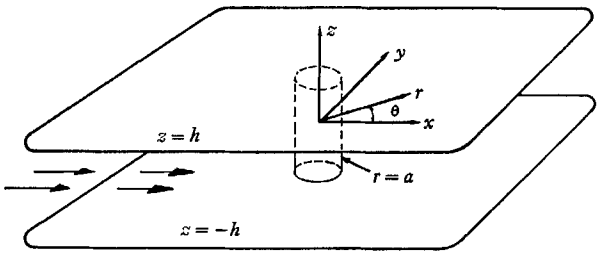

FIGURE 1. Notations.

Thus the Stokes solution of Hele-Shaw flow is not exact. On the other hand, Stokes argued that the error is sensible only in a region right next to the cylinder and that, at a distance further away from the cylinder than the thickness of the sheet, the approximation should be good.

Thompson (1968) used the method of singular perturbation to investigate the flow when the sheet-thickness-to-post-diameter ratio, h/a, is much smaller than 1. In this case, the field may be divided into two regions: an outer region, in which the velocity gradient in the plane of the plates is much smaller than that normal to the plates, and an inner region, where all velocity gradients are of the same order of magnitude. Thompson shows that the thickness of the inner region is of the order of the thickness of the sheet, h. Appropriate solutions in these two regions are matched in their range of common validity. The solution is expressed in power series of the thickness ratio up to $(h/a)^2$.

In the pulmonary alveoli, however, the thickness ratio, h/a, is about 2 or 3. Thus, neither Stokes's nor Thompson's solution is applicable. In this paper, a uniformly valid solution is constructed in the form of an infinite series, the general terms of which satisfy the equations of motion, continuity, and the no-slip condition on the plates. The boundary condition at infinity is assumed to be a Poiseuille flow in the x-direction, Hence the sum of the series is made to tend to the Poiseuille solution at infinity. On the post surface the solution is expanded into a series of orthogonal functions. The coefficients of the expansion are set to zero when the no-slip condition is imposed. From this, all unknown constants are determined. It will be shown that the series is adequate for practical computation when $h/a \leqslant 5$; and the velocity distribution and resistance to the flow have been calculated numerically for $h/a = 0{\cdot}1$, 1 and 5.

An approximate solution, which consists of the first two terms of the series, is evaluated to show that it furnishes a good approximation to the flow resistance when h is not greater than a. In a companion paper, Lee (1969), the approximate solution is extended to construct a flow between two parallel plates interposed with a regular array of posts. When $h/a \to 0$, the approximate solution can be expanded in power series of h/a, and it will be shown that the zeroth- and the first-order terms compare favourably with those obtained by Thompson.

2. Method of solution

Let (r, θ, z) be a set of the cylindrical co-ordinates; let (x, y, z) be a set of Cartesian co-ordinates, with a common z-axis which is the centre-line of the post; and with a common origin which is located midway between the plates. In these co-ordinate systems, the surface of the post is described by $r = a$, while the inner surfaces of the plates are $z = \pm h$ (see figure 1).

The fluid velocity $\mathbf{v}(v_x, v_y, v_z)$ must satisfy the no-slip condition on the surfaces of the post and the plates

$$\mathbf{v} = 0 \quad \text{at} \quad r = a, \tag{1}$$

$$\mathbf{v} = 0 \quad \text{at} \quad z = \pm h. \tag{2}$$

The flow at infinity is assumed to be a uniform Poiseuille flow. Therefore

$$\mathbf{v} = U(1 - z^2/h^2)\,\mathbf{i} \quad \text{as} \quad r \to \infty, \tag{3}$$

where $\mathbf{i}$ is the unit vector in the x-direction and U is the velocity in the midplane $z = 0$ at large distance from the post.

The Reynolds number of the flow will be assumed to be very small, so that the equation of motion is the Stokes equation,

$$\nabla^2 \mathbf{v} = (1/\mu)\,\nabla p, \tag{4}$$

in which μ is the viscosity and p is the pressure. The continuity equation for an incompressible fluid is

$$\nabla . \mathbf{v} = 0. \tag{5}$$

Equations (4) and (5) together show that p is a harmonic function and $\mathbf{v}$ is a biharmonic function.

To solve the problem, we shall first construct a general solution of the differential system (4), (5) and (2). A summation of these general solutions with arbitrary constant multipliers is also a general solution. On this sum, the boundary conditions (1) and (3) can be imposed to determine the unknown constants.

The solution of the differential system (4), (5) and (2) is the sum of (i) biharmonic functions and (ii) harmonic functions. These will now be discussed briefly.

(i) *Biharmonic solutions satisfying* $\nabla^4 \mathbf{v} = 0$

According to Almansi's theorem (Fung 1965, p. 207), any biharmonic vector function $\mathbf{v}$ can be represented in the form

$$\mathbf{v} = z\mathbf{v}_1 + \mathbf{v}_2, \tag{6}$$

in which $\mathbf{v}_1$ and $\mathbf{v}_2$ are harmonic functions. Now, if $\phi_n(x, y)$ and $\overline{\phi}_n(x, y)$ are any two solutions of the differential equation

$$\frac{\partial^2 \phi_n}{\partial x^2} + \frac{\partial^2 \phi_n}{\partial y^2} - \alpha_n^2 \phi_n = 0, \tag{7}$$

where α_n is a constant, then the functions

$$\phi_n(x,y)\cos\alpha_n z, \quad \overline{\phi}_n(x,y)\sin\alpha_n z \tag{8}$$

must be harmonic. Hence (2) will certainly be satisfied in the z-component if v_z takes the form

$$v_z = \phi_n(x,y)\,q_n(z), \tag{9}$$

where

$$q_n(z) = \frac{\sin\alpha_n z}{\sin\alpha_n h} - \frac{z\cos\alpha_n z}{h\cos\alpha_n h}. \tag{10}$$

Substituting (9) into (4), (5), and solving for v_x, v_y and p, one finds

$$\left.\begin{aligned} v_x &= -\frac{1}{\alpha_n^2}\frac{\partial\phi_n}{\partial x}\frac{dq_n}{dz}, \\ v_y &= -\frac{1}{\alpha_n^2}\frac{\partial\phi_n}{\partial y}\frac{dq_n}{dz}, \\ p &= -\frac{2\mu}{h}\phi_n\frac{\cos\alpha_n z}{\cos\alpha_n h}. \end{aligned}\right\} \tag{11}$$

The no-slip conditions $v_x(\pm h) = v_y(\pm h) = 0$ are satisfied if α_n satisfies the following characteristic equation:

$$\sin 2\alpha_n h = 2\alpha_n h. \tag{12}$$

Approximate values of $2\alpha_n h$ are $(2n+\frac{1}{2})\pi \pm i\log(4n+1)\pi$, $n = 1, 2, \ldots$.

All roots of (12) are complex-valued except $\alpha_0 = 0$, which corresponds to

$$\left.\begin{aligned} v_x &= \frac{\partial\phi_0}{\partial x}\left(1-\frac{z^2}{h^2}\right), \\ v_y &= \frac{\partial\phi_0}{\partial y}\left(1-\frac{z^2}{h^2}\right), \\ v_z &= 0, \quad p = -\frac{2\mu}{h^2}\phi_0, \end{aligned}\right\} \tag{13}$$

where $\phi_0(x,y)$ is a harmonic function. For the particular solution (13), the velocity can also be derived from a function $\overline{\psi}_0(x,y)$ such that

$$\left.\begin{aligned} v_x &= -\frac{\partial\overline{\psi}_0}{\partial y}\left(1-\frac{z^2}{h^2}\right), \\ v_y &= \frac{\partial\overline{\psi}_0}{\partial x}\left(1-\frac{z^2}{h^2}\right), \end{aligned}\right\} \tag{14}$$

and $\psi_0(x,y)$ will be the harmonic conjugate of $\phi_0(x,y)$. Thus this solution may also be derived from a complex potential

$$\Phi(Z) = \phi_0 + i\overline{\psi}_0, \tag{15}$$

in which Φ is an analytic function of the complex variable $Z = x+iy$. Equations (13) and (14) constitute Stokes's solution for Hele-Shaw flow.

(ii) *Harmonic solutions satisfying* $\nabla^2\mathbf{v} = 0, p = 0$

By (8), an harmonic solution, which satisfies (2), (4) and (5), is of the form

$$\left.\begin{aligned} v_x &= -\frac{\partial \psi_n}{\partial y}\cos k_n z, \\ v_y &= \frac{\partial \psi_n}{\partial x}\cos k_n z, \\ v_z &= p = 0, \end{aligned}\right\} \tag{16}$$

where $k_n = (2n+1)\pi/2h$ with $n = 0,1,2,\ldots$ and $\psi_n(x,y)$ are the functions listed in (7) with α_n replaced by k_n.

A general solution for the flow should now be expressible in series over all the solutions given in (9), (11) and (16), and upon transforming these to cylindrical co-ordinates, we obtain

$$v_r = \frac{\partial \phi_0(r,\theta)}{\partial r}\left(1-\frac{z^2}{h^2}\right) - \mathrm{Re}\left[\sum_{n=1}^{\infty}\frac{1}{\alpha_n^2}\frac{\partial \phi_n(r,\theta)}{\partial r}\frac{dq_n(z)}{dz}\right] - \sum_{n=0}^{\infty}\frac{1}{r}\frac{\partial \psi_n(r,\theta)}{\partial \theta}\cos k_n z, \tag{17}$$

$$v_\theta = \frac{1}{r}\frac{\partial \phi_0(r,\theta)}{\partial \theta}\left(1-\frac{z^2}{h^2}\right) - \mathrm{Re}\left[\sum_{n=1}^{\infty}\frac{1}{\alpha_n^2 r}\frac{\partial \phi_n(r,\theta)}{\partial \theta}\frac{dq_n(z)}{dz}\right] + \sum_{n=0}^{\infty}\frac{\partial \psi_n(r,\theta)}{\partial r}\cos k_n z, \tag{18}$$

$$v_z = \mathrm{Re}\left[\sum_{n=1}^{\infty}\phi_n(r,\theta)\,q_n(z)\right], \tag{19}$$

$$p = -\frac{2\mu}{h}\left\{\frac{\phi_0(r,\theta)}{h} + \mathrm{Re}\left[\sum_{n=1}^{\infty}\phi_n(r,\theta)\frac{\cos \alpha_n z}{\cos \alpha_n h}\right]\right\}. \tag{20}$$

The functions ϕ_n and ψ_n are solutions of (7), which is well known. The function ϕ_0 can be taken as any linear combinations of the following:

$$r^s\cos s\theta, \quad r^s\sin s\theta, \quad r^{-s}\cos s\theta, \quad r^{-s}\sin s\theta, \tag{21}$$

Similarly, $\phi_n(r,\theta)$ can be taken as any linear combinations of

$$\left.\begin{aligned} &I_s(\alpha_n r)\cos s\theta, \quad I_s(\alpha_n r)\sin s\theta, \\ &K_s(\alpha_n r)\cos s\theta, \quad K_s(\alpha_n r)\sin s\theta; \end{aligned}\right\} \tag{22}$$

and $\psi_n(r,\theta)$ can be taken as any linear combinations of

$$\left.\begin{aligned} &I_s(k_n r)\cos s\theta, \quad I_s(k_n r)\sin s\theta, \\ &K_s(k_n r)\cos s\theta, \quad K_s(k_n r)\sin s\theta, \end{aligned}\right\} \tag{23}$$

where $s = 0,1,2,\ldots$ and I_s, K_s are modified Bessel functions of the first and second kind of order s respectively. By virtue of the boundary condition (3), terms involving r^s $(s > 1)$, $I_s(\alpha_n r)$ and $I_s(k_n r)$ for $s \geqslant 0$ must be excluded. For $K_s(\alpha_n r)$ to be admissible, $\mathrm{Re}\,(\alpha_n) > 0$ is required.

3. Flow around a circular post

For a circular post, it is sufficient to give an exact solution by taking $s = 1$. Hence (17), (18), (19) and (20) become

$$v_r = \left\{\left(U + b\frac{a^2}{r^2}\right)\left(1 - \frac{z^2}{h^2}\right) - \mathrm{Re}\left[\sum_{n=1}^{\infty} \frac{A_n + iB_n K_1'(\alpha_n r)}{\alpha_n \quad K_1(\alpha_n a)} \frac{dq_n(z)}{dz}\right] - \sum_{n=0}^{\infty} \frac{c_n}{k_n r} \frac{K_1(k_n r)}{K_1(k_n a)} \cos k_n z\right\} \cos\theta, \tag{24}$$

$$v_\theta = \left\{\left(-U + b\frac{a^2}{r^2}\right)\left(1 - \frac{z^2}{h^2}\right) + \mathrm{Re}\left[\sum_{n=1}^{\infty} \frac{A_n + iB_n K_1(\alpha_n r)}{\alpha_n^2 r \quad K_1(\alpha_n a)} \frac{dq_n(z)}{dz}\right] + \sum_{n=0}^{\infty} \frac{c_n K_1'(k_n r)}{K_1(k_n a)} \cos k_n z\right\} \sin\theta, \tag{25}$$

$$v_z = \mathrm{Re}\left\{\sum_{n=1}^{\infty} (A_n + iB_n) \frac{K_1(\alpha_n r)}{K_1(\alpha_n a)} q_n(z)\right\} \cos\theta, \tag{26}$$

$$p = p_0 - \frac{2\mu}{h}\left\{\left(\frac{Ur}{h} - b\frac{a^2}{rh}\right) + \mathrm{Re}\left[\sum_{n=1}^{\infty} (A_n + iB_n) \frac{K_1(\alpha_n r)}{K_1(\alpha_n a)} \frac{\cos\alpha_n z}{\cos\alpha_n h}\right]\right\} \cos\theta. \tag{27}$$

Here b, c_0, c_1, ..., A_1, B_1, ..., p_0 are unknown real constants. Because all terms vanish at infinity, except the first terms in v_r and v_θ, (24), (25) and (26) satisfy the boundary condition (3). The unknown constants can be determined by (1).

As $\cos k_n z$ forms a complete set of orthogonal functions in the interval $(0, h)$, we can expand the velocities v_r and v_θ at $r = a$ into a half-range Fourier series. Since

$$1 - \frac{z^2}{h^2} = \sum_{m=0}^{\infty} d_m \cos k_m z, \tag{28}$$

$$-\frac{1}{\alpha_n}\frac{dq_n}{dz} = \sum_{m=0}^{\infty} e_{nm} \cos k_m z, \tag{29}$$

where
$$d_m = \frac{32(-1)^m}{\pi^3(2m+1)^3} \quad \text{and} \quad e_{nm} = \frac{4(-1)^m k_m \alpha_n}{h^2(\alpha_n^2 - k_m^2)^2}, \tag{30}$$

v_r and v_θ from (24), (25) can be reduced into the following forms:

$$v_r = \sum_{n=0}^{\infty} C_n(r) \cos\theta \cos k_n z, \tag{31}$$

$$v_\theta = \sum_{n=0}^{\infty} D_n(r) \sin\theta \cos k_n z. \tag{32}$$

Then the no-slip condition on the surface of the post $r = a$ requires that

$$C_n(a) = 0, \quad D_n(a) = 0 \quad (n = 0, 1, 2, \ldots). \tag{33}$$

As to v_z, the coefficients in the series in (26) are not easy to determine: the functions $q_1(z)$, $q_2(z)$ ... are not orthogonal in the range $(-h \leqslant z \leqslant h)$. As v_z is an odd function in z, one could expand v_z into a Fourier series in $\sin k_n z$. However, for k_n selected above, $\sin k_n z$ does not vanish at $z = \pm h$, and so the boundary

condition $v_z(\pm h) = 0$ would not be satisfied by the individual terms. To improve the situation, we introduce a set of orthonormal functions $Y_n(z)$, which were used by Gaydon & Shepherd (1964) in an analogous problem in elasticity

$$Y_n(z) = \frac{1}{\sqrt{2}}\left\{\frac{\sin\lambda_n z}{\sin\lambda_n h} - \frac{\sinh\lambda_n z}{\sinh\lambda_n h}\right\}, \tag{34}$$

where λ_n is a positive eigenvalue of the characteristic equation

$$\tan\lambda_n h = \tanh\lambda_n h. \tag{35}$$

Approximately, $$\lambda_n = (n+\tfrac{1}{4})(\pi/h), \quad \text{for} \quad n = 1, 2, 3, \ldots. \tag{36}$$

Note that $$Y_n(\pm h) = Y_n'(\pm h) = 0, \tag{37}$$

so that, if v_z is expanded into a generalized Fourier series,

$$v_z = \sum_{n=1}^{\infty} E_n(r)\cos\theta Y_n(z). \tag{38}$$

The boundary condition $v_z(\pm h) = 0$ is now satisfied identically. The boundary condition $v_z|_{r=a} = 0$ requires that

$$E_n(a) = 0 \quad (n = 1, 2, 3\ldots). \tag{39}$$

It will be seen that (33) and (39) furnish the correct number of equations for the determinations of the unknown constants b, c_0, c_1,..., A_1, B_1, ...

The expansion of $q_m(z)$ in terms of $Y_n(z)$ is given by

$$q_m(z) = \sum_{n=1}^{\infty} f_{mn} Y_n(z), \tag{40}$$

where $$f_{mn} = \frac{8\sqrt{2}\,\lambda_n^3\alpha_m^3}{h^2(\lambda_n^4 - \alpha_m^4)^2}\left[\tan\alpha_m h\coth\lambda_n h - \frac{\alpha_m}{\lambda_n}\right]. \tag{41}$$

4. Numerical calculations

If we truncate the series (31), (32) and (38) by replacing the upper limit of the summations by N, then the conditions (33) and (39) furnish $3N+2$ algebraic equations connecting the $3N+2$ unknowns b, c_0, c_1, ..., c_N; A_1, A_2, ..., A_N; B_1, B_2, ..., B_N. These algebraic equations are

$$\begin{aligned}
bd_n + \mathrm{Re}\left[\sum_{m=1}^{N}\frac{(A_m + iB_m)K_1'(\alpha_m a)}{K_1(\alpha_m a)}e_{mn}\right] - \frac{c_n}{k_n a} &= -Ud_n \quad (n = 0, \ldots, N),\\
bd_n - \mathrm{Re}\left[\sum_{m=1}^{N}\frac{A_m + iB_m}{\alpha_m a}e_{mn}\right] + c_n\frac{K_1'(k_n a)}{K_1(k_n a)} &= Ud_n \quad (n = 0, \ldots, N),\\
\mathrm{Re}\left[\sum_{m=1}^{N}(A_m + iB_m)f_{mn}\right] &= 0 \quad (n = 1, \ldots, N),
\end{aligned} \tag{42}$$

where d_n, e_{mn} and f_{mn} are given in (30) and (41).

Equations (42) have been solved on a high speed computer for a number of representative values of the parameter h/a. The number N is chosen according

to the following criteria: (i) the boundary values of $v_r|_{r=a}$, $v_\theta|_{r=a}$, $v_z|_{r=a}$ which should be zero, must tolerate an error no greater than 0·0005 times the undisturbed velocity U, (ii) the coefficients c_n, A_n, B_n become small for sufficiently large n; the last terms c_N, A_N, B_N must be smaller than 0·0005 times U. For example, when $h/a = 1$, one requires $N = 15$. When $h/a = 5$, one must have $N = 25$.

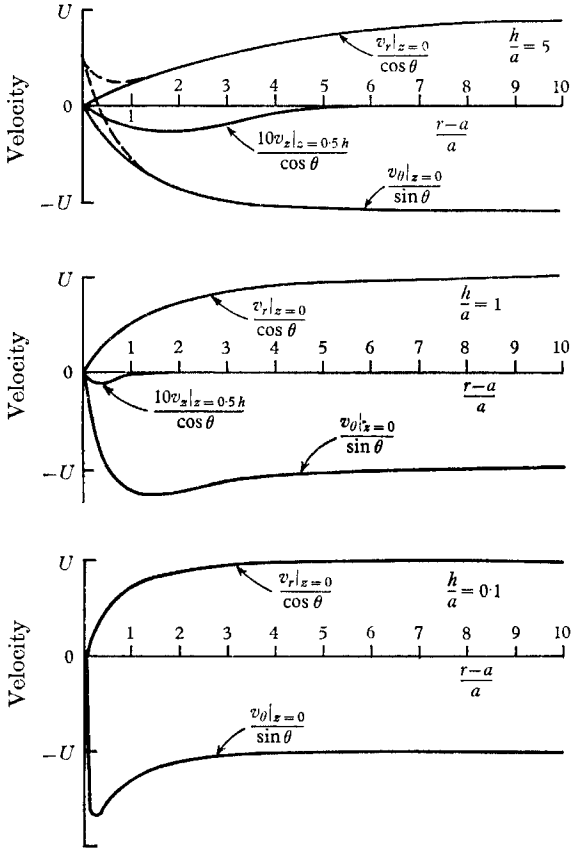

FIGURE 2. Velocity distributions *vs.* $(r-a)/a$ for the cases $h/a = 5$, 1 and 0·1.

In figure 2 the functions $v_r/\cos\theta$ and $v_\theta/\sin\theta$ at $z = 0$ and 10 times $v_z/\cos\theta$ at $z = 0{\cdot}5h$ are plotted for three cases: (*a*) $h/a = 5 (N = 25)$,† (*b*) $h/a = 1$ $(N = 15)$ and (*c*) $h/a = 0{\cdot}1$ $(N = 10)$. These functions are directly proportional to the velocity distributions. They are plotted against the dimensionless parameter, $(r-a)/a$, which is the distance to the cylinder expressed in units of cylinder radius. The v_θ distribution is seen to depend very much on the thickness ratio h/a. It suggests that v_θ increases from zero to a maximum value in distance of the order of h from the cylinder, and that the maximum value of v_θ decreases as h/a increases. To show this more clearly, $v_\theta/\sin\theta$ and $v_r/\cos\theta$ at $z = 0$ for the case $h/a = 0{\cdot}1$ are plotted against the parameter $(r-a)/h$ in figure 3. From

† The N given in the parenthesis may not be the smallest N which satisfies the criteria of numerical truncation named above.

figures 2 and 3 we see that, if h/a is small, very rapid change in v_θ takes place in the vicinity of the post. Such a rapid change in velocity is not indicated for the radial velocity v_r. When the three cases shown in figure 2 are compared, one sees that v_r rises more slowly with r/a for larger h/a.

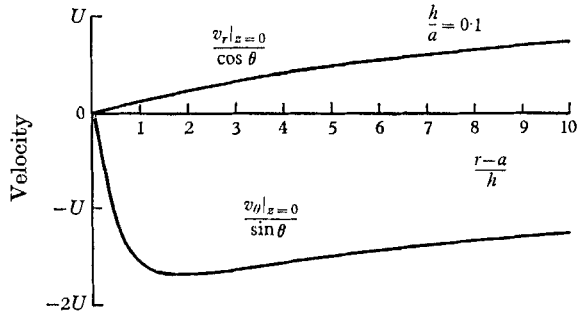

FIGURE 3. Velocity distributions *vs.* $(r-a)/h$ for the case $h/a = 0{\cdot}1$.

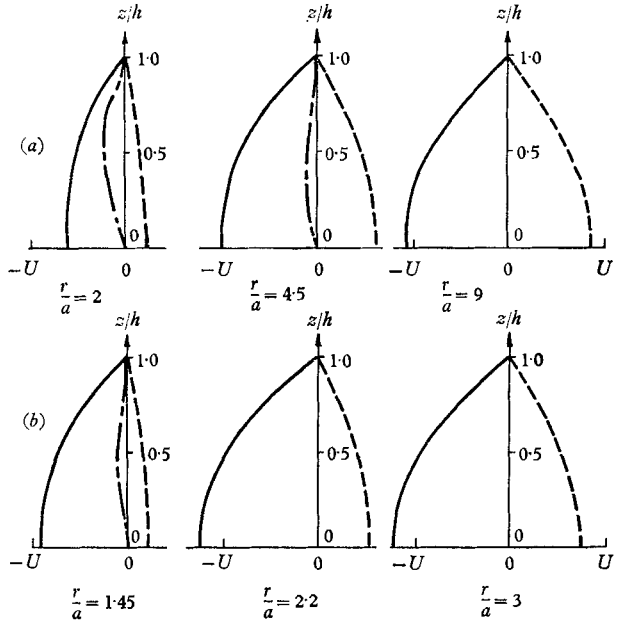

FIGURE 4. Velocity profiles in the z direction at several radial stations. (*a*) $h/a = 5$; (*b*) $h/a = 1$. ——, $v_\theta/\sin\theta$; - - - -, $v_r/\cos\theta$; -·-·-, $10v_z/\cos\theta$.

The velocity component of v_z is seen to be very small compared with v_r and v_θ. Note that the scale for v_z is magnified 10 times in figure 2, as compared with v_r, v_θ. v_z is significant only within a distance about h from the surface of the cylinder. For $h/a = 0{\cdot}1$, $|v_z|$ is less than $0{\cdot}002U$, and is too small to be plotted.

In figure 4 velocity profiles at certain radii are plotted against z for $h/a = 5$ and 1. The case $h/a = 0{\cdot}1$ is not presented, because in that case the velocity profiles for v_r and v_θ are nearly parabolic also at larger h/a. The profile for v_z is described mainly by the eigenfunction $q_1(z)$ and not parabolic.

5. Resistance to flow

The drag acting on the post is

$$D = \int_{-h}^{h} \int_{0}^{2\pi} (p_{rr} \cos\theta - p_{r\theta} \sin\theta)_{r=a} \, a \, d\theta \, dz,$$

$$= \frac{4\pi\mu U a^2}{h} \left\{ 1 - b + \frac{h}{2a} \left[\sum_{n=0}^{\infty} (-1)^n c_n \right] + \mathrm{Re} \left[\Sigma \frac{h(A_n + iB_n)}{a \cos^2 \alpha_n h} \right] \right\}, \tag{43}$$

where $$p_{rr} = -p + 2\mu \frac{\partial v_r}{\partial r} \quad \text{and} \quad p_{r\theta} = \mu \left(\frac{\partial v_\theta}{\partial r} - \frac{v_\theta}{r} + \frac{1}{r} \frac{\partial v_r}{\partial \theta} \right)$$

are the normal and shear stresses at the post surface respectively. The drag force acting on the post can be expressed by a dimensionless coefficient

$$f_D = \frac{\mathrm{D}}{4\pi\mu U h}, \tag{44}$$

which is a function of the dimensionless parameter h/a.

Due to the presence of the post, the stresses on the plates are modified by comparison with those for pure Poiseuille flow. The total additional resistance of the flow is not the drag acting on the post alone, but can be computed by a summation of all the perturbation forces acting on a cylindrical surface at very large radius concentric with the post. At such a surface $r = r_0$ with $r_0 \to \infty$, perturbed strain rates and momentum fluxes are at most of the order of $1/r_0^3$, while perturbed pressure is of the order of $1/r_0$. Thus the resistance of the flow is solely due to the pressure over the surface $r = r_0$:

$$F_R = -\int_{-h}^{h} \int_{0}^{2\pi} p|_{r=r_0} \, r_0 \cos\theta \, d\theta \, dz = \frac{4\pi\mu U a^2}{h} \left(\frac{r_0^2}{a^2} - b \right). \tag{45}$$

The first term in the parentheses is the resistance of pure Poiseuille flow. The second term is the additional resistance due to the presence of the post. We shall define a dimensionless coefficient f_R for the 'additional' resistance as follows:

$$f_R = \frac{F_R}{4\pi\mu U h} - \frac{r_0^2}{h^2} = -\frac{a^2}{h^2} b. \tag{46}$$

In figure 4, f_D and f_R are plotted against h/a. As f_D and f_R respectively represent the drag on the post and the additional resistance on the post and the plates due to the presence of the post, the figure shows that for the same h the drag and resistance at first drop quickly as the radius of the post decreases and then gradually level off to small values.

Figure 4 also shows that f_D is about twice f_R. Their difference is equal to the force acting on the plates. This force is

$$F_W = 2 \int_{0}^{2\pi} \int_{a}^{r_0} (p_{xz}|_{z=h}) \, r \, dr \, d\theta,$$

$$= -\frac{4\pi\mu U a^2}{h} \left\{ \frac{r_0^2}{a^2} - 1 - \frac{h}{2a} \sum_{n=0}^{\infty} (-1)^n c_n - \mathrm{Re} \left[\sum_{n=1}^{\infty} \frac{h(A_n + iB_n)}{a \cos^2 \alpha_n h} \right] \right\}, \tag{47}$$

where $p_{xz} = \mu(\partial v_z/\partial x + \partial v_x/\partial z)$. Of course, as it is expected, $D - F_R - F_W = 0$.

6. The two-term approximation

When we take $N = 0$, (42) is reduced to two equations, from which the constants b and c_0 can be determined. We shall call this the two-term approximation.

$$v_r = U\cos\theta\left\{\left(1-\frac{K_2(ka)}{K_0(ka)}\frac{a^2}{r^2}\right)\left(1-\frac{z^2}{h^2}\right)+\frac{2}{kr}\frac{K_1(kr)}{K_0(ka)}\frac{32\cos kz}{\pi^3}\right\}, \tag{48}$$

$$v_\theta = -U\sin\theta\left\{\left(1+\frac{K_2(ka)}{K_0(ka)}\frac{a^2}{r^2}\right)\left(1-\frac{z^2}{h^2}\right)+\frac{2K_1'(kr)}{K_0(ka)}\frac{32\cos kz}{\pi^3}\right\}, \tag{49}$$

$$v_z = 0, \tag{50}$$

$$p = p_0-\frac{2\mu U}{h^2}\left(r+\frac{K_2(ka)}{K_0(ka)}\frac{a^2}{r}\right)\cos\theta, \tag{51}$$

where $k = k_0 = \pi/2h$. This solution satisfies the differential equations and the boundary conditions at infinity and on the plates. The only condition that may be violated is the no-slip condition on the surface of the post. Therefore, an evaluation of the values of v_r and v_θ on $r = a$, will indicate the accuracy of the solution. When we put $r = a$ in (48) and (49), we obtain

$$\left.\begin{aligned} v_r &= -2U\cos\theta\frac{K_1(ka)}{kaK_0(ka)}\left\{1-\frac{z^2}{h^2}-\frac{32}{\pi^3}\cos kz\right\},\\ v_\theta &= -2U\sin\theta\frac{K_1'(ka)}{K_0(ka)}\left\{1-\frac{z^2}{h^2}-\frac{32}{\pi^3}\cos kz\right\}, \end{aligned}\right\} \tag{52}$$

upon using the recurrence relations of modified Bessel functions. A simple calculation shows that

$$\left|1-\frac{z^2}{h^2}-\frac{32}{\pi^3}\cos kz\right| \leqslant 0{\cdot}043 \quad \text{for all} \quad |z| \leqslant h. \tag{53}$$

Hence the maximum errors of the approximate solution at $r = a$ are

$$\left.\begin{aligned} \max\left|\frac{v_r}{\cos\theta}\right|_{r=a} &\leqslant \frac{0{\cdot}086K_1(ka)U}{K_0(ka)\,ka},\\ \max\left|\frac{v_\theta}{\sin\theta}\right|_{r=a} &\leqslant \frac{0{\cdot}086K_1'(ka)U}{K_0(ka)}. \end{aligned}\right\} \tag{54}$$

The right-hand side of (54) is small if h/a is small (ka large), and is large if h/a is large (ka small). Hence the approximate solution is valid when h/a is small. For the limiting case $h/a \to 0$ ($ka \to \infty$), the error is bounded by $0{\cdot}086U/ka$ or $0{\cdot}086U$. For $h/a = 0{\cdot}1$, 1 and 5, the errors of the approximate solutions at $r = a$ and $z = 0$ are

h/a	$\left\lvert\frac{\Delta v_r}{U\cos\theta}\right\rvert$	$\left\lvert\frac{\Delta v_\theta}{U\sin\theta}\right\rvert$	R/h
5·0	0·45	0·51	4·0
1·0	0·052	0·12	1·5
0·1	0·004	0·068	1·03

in which Δ indicates the error of the argument. In the last column R is the radius beyond which $\Delta v_r|_{z=0}$ and $\Delta v_\theta|_{z=0}$ are smaller than 0·01 times U. In figure 2 the approximate solutions are plotted as dotted lines. We see that in the case $h/a = 5$ the approximate solution is poor in the neighbourhood of the cylinder within a distance of about one radius. In the cases $h/a = 1$ and 0·1, the difference between the approximate and exact solutions cannot be exhibited clearly in the figure.

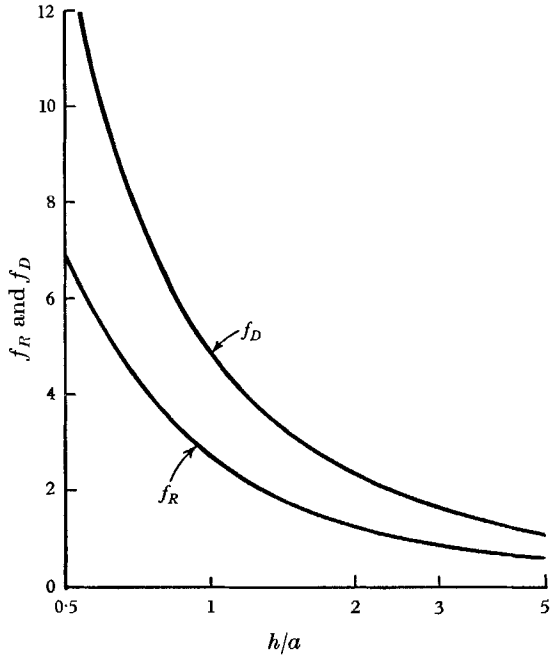

FIGURE 5. The dimensionless coefficients f_D representing the drag force acting on the post and f_R representing the total resistance over and above the Poiseuillian value as functions of the h/a ratio.

Equally good agreement with the exact theory is also shown in calculating the drag and resistance of the system. By retaining only the terms associated with b and c_0 in (43) and (46), one obtains

$$f_D = \frac{a^2}{h^2}\left(1 + \frac{K_2(ka)}{K_0(ka)} + \frac{16}{\pi^2 ka}\frac{K_1(ka)}{K_0(ka)}\right), \quad f_R = \frac{a^2 K_2(ka)}{h^2 K_0(ka)}. \tag{55}$$

These approximate equations give values of f_D and f_R 0·5 % larger than the exact ones of (44) and (46) when $h/a = 1$ and 2·4 % when $h/a = 5$. As modified Bessel functions are always positive, (55) shows that $f_D > f_R$ is valid for all h/a.

With the help of (14) and (16), we can construct a stream function for the approximate velocities in (48) and (49). Calculated patterns of streamlines are plotted in figure 5 for $h/a = 5$, 1 and 0·1. These patterns are independent of z to the accuracy indicated in (54). Comparing the velocity distributions given in figure 2, one sees that, for larger values of h/a, more fluid is slowed down by the presence of the post. This fact is demonstrated in figure 6, which shows that the

streamlines, generated from the same position at infinity, are deflected further away from the post as the ratio h/a increases.

Let us expand the solution (48), (49) and (51) into an asymptotic series in $1/ka$ when $ka \to \infty$ (i.e. $h \to 0$). Using the asymptotic expansions for modified Bessel functions, replacing the term $32\cos kz/\pi^3$ in the velocities by $1-z^2/h^2$, and retaining only terms up to the first order $1/ka$, one obtains

$$v_r = U\cos\theta\left(1-\frac{z^2}{h^2}\right)\left\{1-\frac{a^2}{r^2}-\frac{2}{ka}\left[\frac{a^2}{r^2}-\left(\frac{a}{r}\right)^{\frac{3}{2}}e^{-k(r-a)}\right]\right\}, \tag{56}$$

$$v_\theta = -U\cos\theta\left(1-\frac{z^2}{h^2}\right)\left\{1+\frac{a^2}{r^2}-2\left(\frac{a}{r}\right)^{\frac{1}{2}}e^{-k(r-a)}+\frac{1}{ka}\left[\frac{2a^2}{r^2}-\frac{1}{4}\left(\frac{a}{r}\right)^{\frac{1}{2}}e^{-k(r-a)}\right]\right\}, \tag{57}$$

$$p = p_0-\frac{2\mu Ua^2}{h^2}\left[\frac{r}{a^2}+\frac{1+2/ka}{r}\right]. \tag{58}$$

The velocity field, after one neglects the exponential term in v_θ and all the first-order terms involving $1/ka$, reduces to the Stokes's solution of Hele-Shaw flow around a circular post. Because the exponential function $\exp[ka(r/a-1)]$ decays rapidly to zero, (57) shows that the velocity v_θ near the post change

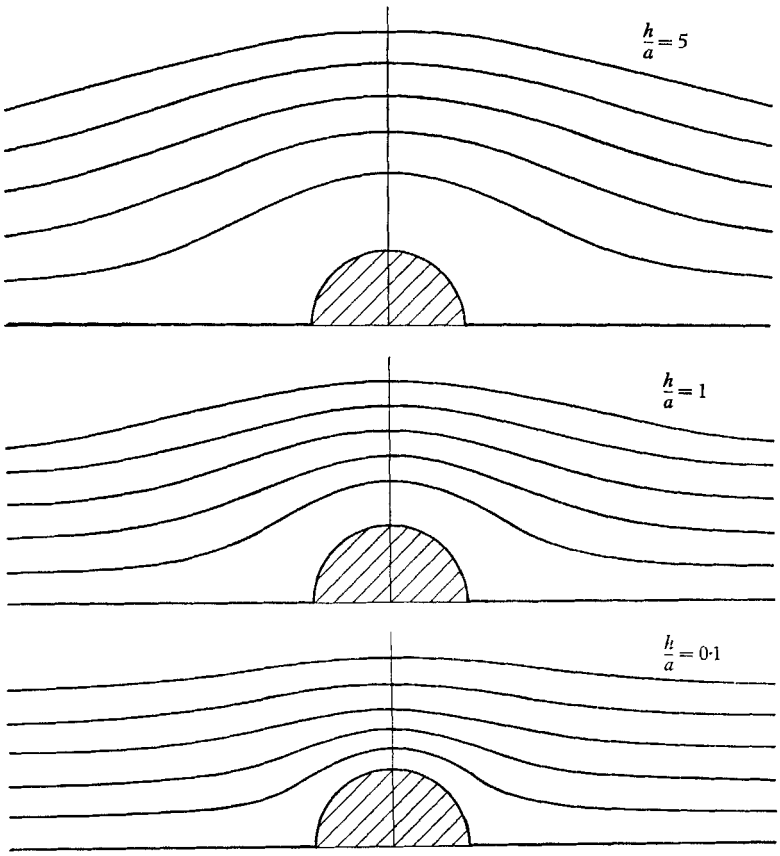

FIGURE 6. Streamline patterns for the cases $h/a = 5$, 1 and 0·1.

sharply in the θ-direction (cf. figure 2). This sharp velocity profile is also demonstrated by the following estimations on velocity gradients

$$\frac{\partial v_\theta}{\partial r} \sim \frac{\partial v_\theta}{\partial z} \sim \frac{\partial v_r}{\partial z} \sim ka\frac{U}{a^2}, \quad \frac{\partial v_r}{\partial r} \sim \frac{U}{a^2}, \tag{59}$$

which are obtained by differentiating (56), (57) and neglecting higher-order terms.

Expansions based on the parameter h/a have also been studied by Thompson, who separated the flow field into an outer region and an inner region as discussed in § 1. Thompson's zeroth- and first-order expansions agree with those of (56), (57) and (58) to the accuracy indicated in (54). Better agreement is obtained for the outer pressure. Thompson gives

$$p = p_0 - 2\mu U a^2[r/a^2 + (1 + 1{\cdot}261h/a)/r]/h^2. \tag{60}$$

This compares favourably with (58), which can be put in the form

$$p = p_0 - 2\mu U a^2[r/a^2 + (1 + 1{\cdot}273h/a)/r]/h^2. \tag{61}$$

7. Conclusions

A method to determine the flow around a single post confined between two parallel plates is presented. The series solution was found to be adequate for numerical computation when the ratio of the distance between the plates, $2h$, and the diameter of the post, $2a$, is not larger than 5. Numerical results indicate that the dimensionless resistance of the flow drops rapidly at first and then gradually levels off as h/a increases. For the flow field around the post, it was found that (*a*) v_θ changes rapidly near the post when h/a is small, (*b*) v_r also rises more rapidly for smaller h/a, and (*c*) v_z is much smaller than v_r, v_θ.

This study was supported by U.S. Air Force Office of Scientific Research, Grant AF-AFOSR-1186-67, National Science Foundation, Grant GK-1415, and San Diego County Heart Association.

REFERENCES

FUNG, Y. C. 1965 *Foundations of Solid Mechanics.* Englewood Cliffs, N.J.: Prentice-Hall.

FUNG, Y. C. & SOBIN, S. S. 1969 *J. Appl. Physiol.* **26**, 472.

GAYDON, F. A. & SHEPHERD, W. M. 1964 *Proc. Roy. Soc.* A **281**, 184.

HELE-SHAW, H. S. 1897 *Trans. Roy. Inst. Nav. Arch.* **41**, 21.

HELE-SHAW, H. S. 1898*a* *Trans. Roy. Inst. Nav. Arch.* **42**, 49.

HELE-SHAW, H. S. 1898*b* *Rep. 68th Mtg. Brit. Ass.* 136.

HELE-SHAW, H. S. & HAY, A. *Phil. Trans.* A **195**, 303.

LEE, J. S. 1969 To appear in *J. Biomechanics.*

LEE, J. S. & FUNG, Y. C. 1968 Paper no. 68-WA/BHF-2, ASME Winter Annual Meeting.

SOBIN, S. S. & FUNG, Y. C. 1967 *Physiologist,* **10**, 308.

STOKES, G. 1898 *Rep. British Assoc.* A **144** (also papers, vol. 3, p. 278).

THOMPSON, B. W. 1968 *J. Fluid Mech.* **31**, 397.